This is the accepted manuscript made available via CHORUS. The article has been published as:

Isotope effect and critical magnetic fields of superconducting math xmlns="http://www.w3.org/1998/Math/MathML">msub>mrow>mi>YH/mi>/mrow>mn>6/mn>/msub>/math>: A Migdal-Eliashberg theory approach

S. Villa-Cortés, O. De la Peña-Seaman, Keith V. Lawler, and Ashkan Salamat

Phys. Rev. B **108**, L020506 — Published 24 July 2023

DOI: 10.1103/PhysRevB.108.L020506

The Isotope Effect and Critical Magnetic Fields of Superconducting YH_6: A Migdal-Eliashberg Theory Approach

S. Villa-Cortés,[1,2,*] O. De la Peña-Seaman,[1] Keith V. Lawler,[2] and Ashkan Salamat[2,3]

[1] *Instituto de Física, Benemérita Universidad Autónoma de Puebla, Apartado Postal J-48, 72570, Puebla, Puebla, México*
[2] *Nevada Extreme Conditions Laboratory, University of Nevada Las Vegas, Las Vegas, Nevada 89154, USA*
[3] *Department of Physics & Astronomy, University of Nevada Las Vegas, Las Vegas, Nevada 89154, USA*

(Dated: July 17, 2023)

The emergence of near-ambient temperature superconductivity under pressure in the metal hydride systems has motivated a desire to further understand such remarkable properties, specifically critical magnetic fields. YH_6 is suggested to be a departure from conventional superconductivity, due to apparent anomalous behavior. Using density functional calculations in conjunction with Migdal-Eliashberg theory we show that in YH_6 the critical temperature and the isotope effect under pressure, as well as the high critical fields, are consistent with strong-coupling conventional superconductivity; a property anticipated to extend to other related systems. Furthermore, the strong-coupling corrections occur to the expected BCS values for the isotope effect coefficient (α), Ginzburg-Landau parameter ($\kappa_1(T)$), London penetration depth ($\lambda_L(T)$), electromagnetic coherence length ($\xi(T)$), and the energy gap (Δ_0).

Keywords: superconductivity, isotope effect, Eliashberg theory, superhydride, high pressure

Over the last decade, a new class of materials of stoichiometric to hydrogen-rich metal hydrides under pressure has emerged with theoretical predictions being made about their crystal structures, electronic, dynamic, and coupling properties [1–4]. As a result of those periodic table spanning predictions [5], several conventional-superconductor candidates have been proposed with critical temperatures (T_c) approaching room temperature [6–8]. The experimental breakthrough for these materials came with the discovery of phonon-mediated superconductivity in H_3S, with a maximum T_c of 203 K measured at 155 GPa [9–11]. Subsequently, high-T_c superconductivity measurements were reported in other compounds such as LaH_{10} with a 250–260 K T_c at 170 GPa [12, 13]; YH_9 with $T_c = 262$ K at 182 GPa [14]; YH_6 with $T_c = 220$ K at approx. 160 GPa [15, 16]; more recently, CaH_6 with $T_c = 215$ K at 172 GPa [17]; as well as a reported carbonaceous sulfur hydride with $T_c = 287$ K at 267 GPa [18, 19]. Most of the theoretical works on the superconducting state of these novel metal hydrides have shown that a strong electron-phonon coupling and high-energy hydrogen phonon modes play a key role in the high T_c calculated values, concluding that they are phonon-mediated strong-coupling superconductors [1–4, 20–32].

Beyond the T_c, there are several other important properties of a superconducting material such as the isotope effect coefficient, the upper, lower, and thermodynamic critical magnetic fields, the penetration depth, and the coherence length. The first has been crucial in elucidating the mechanism responsible for Cooper-pair formation in conventional superconductors. While the last gives us the response of the materials to an external magnetic field. The lower and upper critical magnetic fields (H_{c1} and H_{c2}) are specially interesting, since they give a measure of the Meissner effect and the magnitude of the external magnetic field at which superconductivity is totally suppressed. Due to experimental difficulties [33], measurements of the critical magnetic fields of the metal hydrides at high pressures have been done only at temperatures near T_c. For example, the reported lower boundaries of critical temperature at which the upper critical magnetic field were measured (as determined by the feasible applied magnetic field) are around $0.73\,T_c$ in LaH_{10} [34], $0.94\,T_c$ in YH_6 [15], and $0.9\,T_c$ also in YH_6 [35]. From that data the slope of $H_{c2}(T)$ is fitted and $H_{c2}(0)$ is extrapolated using the Ginzburg-Landau (GL) [36] or the WerthamerHelfand-Hohenberg (WHH) [37] models, giving rise to different values of $H_{c2}(0)$. For example, the reported $H_{c2}(0)$ values for YH_6, the aim of this work, are 107(157) T and 76(102) T at 160 GPa and 200 GPa, respectively, for GL(WHH) [15, 35]. Similar differences are reported in other metal hydrides [9, 12, 33]. Furthermore, these extrapolated values of $H_{c2}(0)$, in conjunction with GL model, Bardeen-Cooper-Schrieffer (BCS) theory [38], and empirical relations [39–42], are used to get a complete description of other relevant quantities, like the critical magnetic fields, penetration depth (λ), coherence length (ξ), as well as the GL parameter ($\kappa = \lambda/\xi$).

While the T_c of the metal hydrides has been widely studied theoretically within a strong-coupling formalism (Migdal-Eliashberg (ME) theory [43]), there are no reports where these other important properties, like the critical magnetic fields and related lengths, are calculated from first principles within a strong-coupling formalism, where corrections to the empirical and weak-coupling values are expected. This, in conjunction with the lack of experimental measurements of the critical fields at low temperatures, has generated confusion and some doubts about the nature of the kind of superconductors they belong to [39–42]. For YH_6, this has even suggested a pos-

* sergio.cortes@unlv.edu, svilla@ifuap.buap.mx

sible deviation from conventional superconductivity [35]. The aim of this communication is to show that the critical magnetic fields, the London penetration depth, and the electromagnetic coherence length can be calculated from first principles using density functional theory (DFT) in conjunction with ME theory [44–58] (for details of the calculations, see Supplemental Material (SM) [59]), showing the conventional nature of YH_6 and providing a general prescription to describe the superconducting state in the high-T_c metal hydrides.

To this end, we start by showing that the behavior of the critical temperature under pressure can be reproduced within the ME formalism, using as input the Eliashberg function ($\alpha^2F(\omega)$) calculated from first principles in the optimized $Im\bar{3}m$ crystal structure. Nuclear effects were taken into account here by means of the zero-point energy through the quasi-harmonic approximation [50, 51], in accordance with the previous evaluation [32] that anharmonic effects are marginal in YH_6 particularly at these pressures (see SM [59] and references therein). As a first step, the Linearized Migdal-Eliashberg Equations (LMEE, Eq. S8 [59]) are solved at a fixed pressure, where T_c is known from experiment. Here, the experimental T_c = 220 K at 160 GPa [15] for YH_6 and T_c = 165 K at 200 GPa [35] for YD_6 are employed as the initial data. From this solution, the functional derivative of T_c with respect to $\alpha^2F(\omega)$ is calculated within the Bergmann and Rainer [60, 61] formalism. These functional derivatives allow a link between the observed changes in $\alpha^2F(\omega)$, by a pressure variation (from P_0 to P_i), to changes in the critical temperature $\Delta T_c(P_0, P_i)$ (Eq. S17 [59]). Fig. 1a shows the behavior of T_c under pressure for both, YH_6 and YD_6. It can be observed that our calculated T_c is in excellent agreement with the experimental values in the whole pressure interval (160 – 330 GPa), and even better than the calculations reported previously in the literature, showing that the behavior of $T_c(P)$ is driven mainly by the changes in the electron-phonon interaction (Fig. S4 [59]). The temperature isotope effect coefficient, α, is calculated by means of the functional derivative of T_c with respect to the Eliashberg Function, taking into account the changes in the electron-electron and the electron-phonon interaction (Eq. S19 [59]), due to the isotope mass substitution, within the Rainer and Culetto [56, 62, 63] formalism. Rather than the usual one-component BCS definition of α, this is a multi-component and fully strong-coupling formalism for the isotope effect coefficient where the effects of the isotopic mass substitution on the whole system (electronic and dynamic properties) are calculated from first principles. Thus, the true effect on T_c due to mass variation of any of the components is fully addressed. Fig. 1b presents α as a function of pressure, also in excellent agreement with experiment. This first step confirms the conventional nature of superconductivity in YH_6 and shows us that the solutions of the gap function, $\tilde{\Delta}_n$, correctly reproduce the superconducting state using the $\alpha^2F(\omega)$ determined from first principles calculations as an input for the LMEEs.

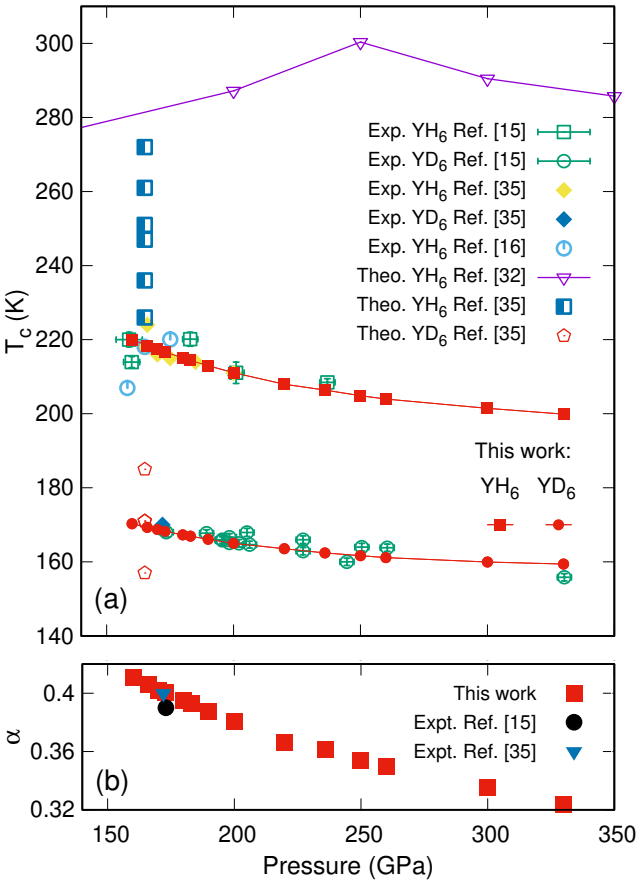


FIG. 1. Calculated $T_c(P)$ for both compounds, YH_6 and YD_6 (a), and the isotope effect coefficient α (b) within the ME formalism (Eqs. (S18) and (S19) in SM [59]). For comparison, it is shown the experimental data, as well as previously reported T_c calculations.

We now focus on the critical magnetic fields, for which the theory has been well known for many years and represents a straightforward derivation from the original Eliashberg equations to include the presence of external magnetic fields [64–67]. In the dirty limit for a strong-coupling superconductor, $H_{c2}(T)$ has to be evaluated from the LMEEs (Eqs. S13 and S14 [59]) in the presence of a homogeneous magnetic field [67] where the pair-breaking parameter $\rho(T)$ and $H_{c2}(T)$ are related by

$$H_{c2}(T) = \rho(T)/eD, \tag{1}$$

$$D = l_{tr}v_F/3, \tag{2}$$

where D is the diffusion constant, v_F the Fermi velocity, l_{tr} the mean free path, and e is the electron charge. Figure 2 shows the temperature dependence of $H_{c2}(T)$ calculated within the ME (Eq. 1, solid lines), GL (dashed lines), and WHH (dotted lines) formalism for YH_6 at 160 and 200 GPa, and YD_6 at 173 GPa. These pressures were selected to make a direct comparison with available

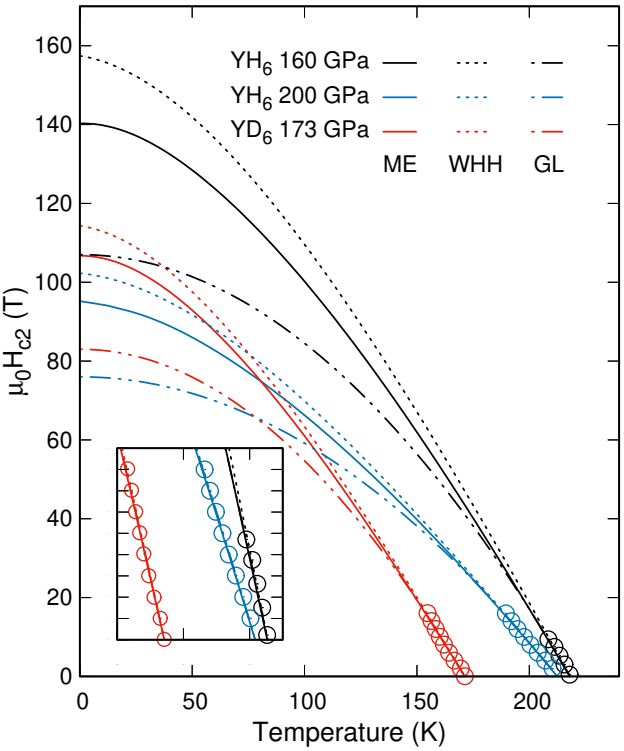


FIG. 2. Calculated upper critical field for both compounds, YH_6 and YD_6, within the Migdal-Eliashberg formalism. For comparison, it is shown the experimental data (symbols) [15, 35] and the extrapolated behavior within the GL and WHH models taken from [15, 35].

experimental data (symbols) [15, 35]. v_F was calculated from the dispersion of the electronic band structure (see Table I), and $l_{tr} = 1.655(1.645)$ Å for $YH_6(YD_6)$ was fitted using Eq. 2 to get the experimental H_{c2} data close to T_c. Near T_c, the calculated values of $H_{c2}(T)$ are similar for the three models and in very good agreement with experiment. As the temperature starts to decrease, the difference between the models' results increases, with the ME results being in between the higher WHH and lower GL values. The largest differences between ME and the GL and WHH models (ΔH_{c2}) are at $T = 0$ K, with values that go from $\Delta H_{c2}(YH_6) = 7(18)$ T at 200 GPa to as high as $\Delta H_{c2}(YH_6) = 17(33)$ T at 160 GPa, in respect to WHH(GL). Although the GL theory is applicable to practically all superconductors, it is a phenomenological theory restricted to temperatures close to T_c. Therefore, GL theory is not expected to give accurate results at lower temperatures, giving rise to the huge differences at T=0 K between itself and the other theories. The WHH formalism is based on weak-coupling BCS theory, and thus should be valid for the whole temperature range; whereas the ME formalism covers weak- and strong-coupling. Thus, the ME results show a distinct strong-coupling correction to the WHH results.

To calculate the thermodynamic critical field, H_c, of an isotropic strong-coupling superconductor, the Non-linear MEEs (NLMEE) have to be solved (Eqs. S5 and S6 [59]). With the knowledge of $\tilde{\Delta}_n$ and $\tilde{\omega}_n$, the difference in free energy between the normal and the superconducting states of the metal, $\Delta F(T) = F_n - F_s$, can be calculated directly. By definition, H_c is given by the relation $H_c(T) = [8\pi(\Delta F(T))]^{1/2}$. Then, from the calculated fields, the GL parameter and the lower critical field can be evaluated from the relations $\kappa_1 = (1/\sqrt{2})H_{c2}/H_c$ and $H_{c1}H_{c2} = H_c^2 \ln(\kappa)$, respectively. Expanding Figure 2 to higher pressures to span the whole pressure range studied, Figure 3 shows the calculated behavior of $H_c(T)$, $H_{c1}(T)$, and $H_{c2}(T)$ for YH_6 (solid lines) and YD_6 (dashed lines) at 160, 200, and 250 GPa. As a function of pressure, there is a steady shift of the critical fields to lower values as the pressure is incremented. In particular, at T=0 K there is a considerable suppression in H_{c2} from 141.5(110.8) T to 111.8(91.0) T for $YH_6(YD_6)$, at 160 and 250 GPa respectively (see Table I). As can be seen, the three fields show an isotopic shift to lower values due to the replacement of hydrogen by deuterium.

The strong-coupling behavior of the calculated $H_{c2}(T)$ and $H_c(T)$ by the ME-model is confirmed by the deviation function, $D(t)$ (Eqs. S27 and S28 [59]), which shows the standard behavior (positive values) for strong-coupling materials, in contrast to the intermediate-coupling behavior (change in sign) that is observed in the WHH model (Fig. S6 [59]). Fig. 3d shows the parameter $\kappa_1(T)$, which has values between approximately 24 and 27 for both compounds at T=0 K (Table I), while at T_c (where κ_1 is similar to the GL κ [68]) this parameter has its minimum values and vary from 17.5 to 17.7. The ratio $\kappa_1(0)/\kappa_1(T_c)$ give us an estimation of the strong-coupling correction to BCS values. While in the weak-coupling formalism there is a universal ratio $\kappa_1(0)/\kappa_1(T_c)$=1.12 [67], the values for $YH_6(YD_6)$ vary from 1.49(1.5) to 1.38(1.4) at 160 and 250 GPa, respectively. Such enhanced values clearly show that these systems are within the strong coupling regime across this noted pressure range, and the slight decrease with respect to pressure shows the tendency towards a less strong-coupling (intermediate) regime, as expected from the general trend under pressure of the coupling parameter (Fig. S4 [59]).

Despite expressions which are valid within Migdal-Eliashberg theory being derived several years ago [69, 70], there are very few strong-coupling superconductor systems with reported numerical results of their electromagnetic properties. Here we are interested in the magnetic field penetration depth (in the London limit) $\lambda_L(T)$, and the electromagnetic coherence length $\xi(T)$. Both quantities are studied in the clean limit, due to the very large energy scale associated with the phonon frequencies and superconducting gap for the metal hydrides, as was previously suggested for H_3S by Nicol and Carbotte [20]. The London-limit penetration depth, which applies when

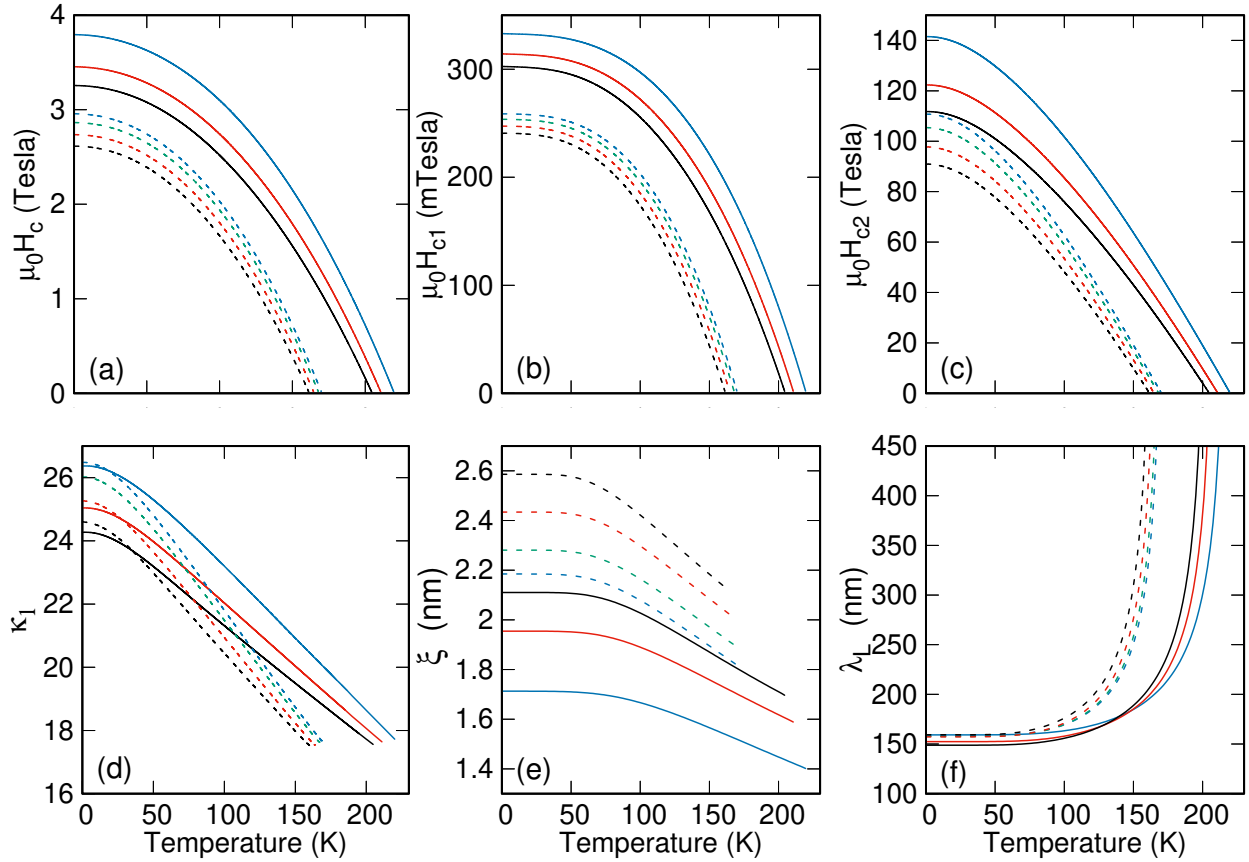


FIG. 3. Calculated thermodynamic (a), lower (b), and upper (c) critical magnetic fields within the Migdal-Eliashberg formalism for YH_6 (solid lines) and YD_6(dashed lines) at 160 (blue), 173 (green), 200 (red), and 250 (black) GPa. The parameter $\kappa_1(T) = (1/\sqrt{2})H_{c2}(T)/H_c(T)$ (d) is used in conjunction with the relation $H_{c1}H_{c2} = H_c^2\ln(\kappa)$ to get the lower critical magnetic field (b). Also shown are the electromagnetic coherence length (e) and the London penetration depth (f) in the clean limit.

$\lambda_L(T) \gg \xi(0)$, is given by

$$\lambda_L(T) = \left[\frac{4}{3}\pi N(0)e^2v_F^2T\mu_0\sum_{n=1}^{\infty}\frac{\tilde{\Delta}_n^2}{\left(\tilde{\omega}_n^2+\tilde{\Delta}_n^2\right)^{3/2}}\right]^{-1/2}, \tag{3}$$

where μ_0 is the permeability and $N(0)$ is the single spin density of electronic states at the Fermi energy. The electromagnetic coherence length, which describes the nonlocality in the electromagnetic response of a superconductor, is given by

$$\xi(T) = \frac{v_F\hbar}{2}\frac{\left[\sum_{n=1}^{\infty}\frac{\tilde{\Delta}_n^2}{\left(\tilde{\omega}_n^2+\tilde{\Delta}_n^2\right)^{3/2}}\right]}{\left[\sum_{n=1}^{\infty}\frac{\tilde{\Delta}_n^2}{\tilde{\omega}_n^2+\tilde{\Delta}_n^2}\right]}. \tag{4}$$

The solutions of the NLMEEs (Eqs. S5 and S6 [59]), $\tilde{\Delta}$ and $\tilde{\omega}$, are required to get both $\lambda_L(T)$ and $\xi(T)$. Numerical results for the temperature variation of $\xi(T)$ are given in Fig. 3e. In superconductors, $\xi(T)$ is the range of the perturbation of the current density caused by an applied electromagnetic field, which is different from the GL coherence length ξ that describes the perturbation of the superconducting pair density. In the weak-coupling theory, both quantities are related at $T = 0$ K through the relation $\xi = 0.739\xi(0)$. From these strong-coupling formalism calculations, $\xi(0)$ is found to be 1.71(2.18) nm and 2.11(2.58) nm for $YH_6(YD_6)$ at 160 and 250 GPa, respectively. Using the GL relation, $\xi = \sqrt{\frac{\phi_0}{2\pi H_{c2}}}$, the GL coherence length ξ is found to be 1.53(1.72) nm and 1.73(1.94) nm for $YH_6(YD_6)$, at the same applied pressures which are in agreement with GL experimental estimations of 1.4–1.8 nm at 160 GPa for YH_6 [15, 35]. These values yield ratios $\xi/\xi(0)$ 0.895(0.787) and 0.82(0.75) for $YH_6(YD_6)$ at 160 and 250 GPa, respectively, which clearly deviate from the weak-coupling limit of 0.739. As the temperature increases, $\xi(T)$ falls quickly near T_c, where the ratio $\xi(T_c)/\xi(0)$ drops to a value of about 0.82(0.83) for $YH_6(YD_6)$ at 160 GPa, which is larger than the BCS value of 0.752 [71].

Fig. 3f shows the temperature dependence of $\lambda_L(T)$. $\lambda_L(0)$ is found to be approximately 159 nm for both, YH_6 and YD_6 at 160 GPa, which is close to the reported BCS values of 164 and 147 nm for H_3S and LaH_{10}, respectively [42]. The strong-coupling deviation function of

TABLE I. Zero-temperature calculated parameters of the superconducting state at selected pressures for YH_6 and YD_6 using the solutions of the NLMEEs and LMEEs, in conjunction with Eqs. 1, 3 and 4 for the upper critical field, London penetration depth (λ_L), and coherence length (ξ), respectively. The critical fields are in units of Tesla, the Fermi velocity (v_F) in $\times 10^5 m/s$ (Eq. S26), λ_L and ξ in nm.

	YH_6							YD_6						
P	v_F	$H_c\,(0)$	$H_{c1}\,(0)$	$H_{c2}\,(0)$	$\kappa_1\,(0)$	$\lambda_L\,(0)$	$\xi\,(0)$	v_F	$H_c\,(0)$	$H_{c1}\,(0)$	$H_{c2}\,(0)$	$\kappa_1\,(0)$	$\lambda_L\,(0)$	$\xi\,(0)$
160	8.76	3.79	0.33	141.5	26.37	159.15	1.712	8.75	2.96	0.26	110.8	26.48	158.38	2.18
180	8.68	3.59	0.33	129.0	25.57	157.98	1.884	8.68	2.83	0.25	103.0	25.76	157.38	2.34
200	8.61	3.45	0.31	122.3	25.04	157.40	1.954	8.59	2.74	0.25	97.7	25.27	157.22	2.43
220	8.53	3.35	0.31	116.7	25.64	158.12	2.164	8.51	2.68	0.25	91.9	24.93	157.93	2.54
250	8.39	3.25	0.30	111.6	24.27	159.04	2.110	8.38	2.61	0.24	90.9	24.60	159.28	2.58

$[\lambda_L(0)/\lambda_L(T)]^{1/2}$ with respect to the two fluid model for YH_6 is shown in Fig. S6 [59]. The deviation function (Eq. S29 [59]), gives a minimum value of -0.05 GPa, which is in contrast to the -0.22 GPa result from BCS weak-coupling theory [72]. By means of Padé approximants [73], the energy gap, Δ_0, can be found from an analytic continuation to the real axis of $\tilde{\Delta}_n$ (computed from the NLMEEs). Here, Δ_0 is 46.68(37.6) meV and 37.7(30.9) meV for $YH_6(YD_6)$ at 160 and 250 GPa, respectively. From these values, the BCS ratios $2\Delta_0/k_BT_c$ are 4.94(5.13) and 4.50(4.74) which shows a strong-coupling correction to the 3.52 BCS value.

To summarize, the superconducting properties and electromagnetic field response of the yttrium hydride YH_6 are computed here from first principles, using DFT in conjunction with ME theory. From these, the experimental behavior of T_c as a function of applied pressure and the isotopic effect can be perfectly reproduced within the harmonic approximation and the strong-coupling formalism for α. Similarly, the calculated $H_{c2}(T)$ with the ME formalism shows excellent agreement with the available experimental data at temperatures near T_c. As T goes to zero, it shows intermediate values between the GL and WHH models, providing an important strong-coupling correction to these currently used phenomenological models. The implemented formalism even allows a full description of the $H-T$ phase diagram by calculating $H_c(T)$, $H_{c1}(T)$, and $\kappa_1(T)$. Finally, the description of the $YH(D)_6$ superconducting state is completed by calculating $\xi(T)$ and $\lambda_L(T)$ within the clean limit, as well as the energy gap Δ_0. From our results, we found that any deviation from BCS behavior is well explained as a strong-coupling correction, and on this basis, we are able to discard any possible anomalous behavior or departure from conventional superconductivity as was previously suggested [35]. Even more, we consider that ME theory, in conjunction with Rainer-Bergmann [67] and Nam's [69, 70] formalism, can provide a general prescription to describe the superconducting state in the high-T_c metal hydrides.

ACKNOWLEDGMENTS

This research is funded in part by the Gordon and Betty Moore Foundation's EPiQS Initiative, Grant GBMF10731, partially supported by the Consejo Nacional de Ciencia y Tecnologa (CONACyT, Mxico) under Grant No. FOP16-2021-01-320399, as well as by the U.S. Department of Energy, Office of Basic Energy Sciences under Award Number DE-SC0020303. The authors thankfully acknowledge computer resources, technical advice, and support provided by Laboratorio Nacional de Supercómputo del Sureste de México (LNS), a member of the CONACYT national laboratories.

[1] L. Zhang, Y. Wang, J. Lv, and Y. Ma, *Materials discovery at high pressures*, Nature Reviews Materials **2**, 17005 (2017).

[2] D. Duan, H. Yu, H. Xie, and T. Cui, *Ab initio approach and its impact on superconductivity*, Journal of Superconductivity and Novel Magnetism **32**, 53–60 (2019).

[3] K. Tanaka, J. S. Tse, and H. Liu, *Electron-phonon coupling mechanisms for hydrogen-rich metals at high pressure*, Phys. Rev. B **96**, 100502 (2017).

[4] T. Bi, N. Zarifi, T. Terpstra, and E. Zurek, in *Reference Module in Chemistry, Molecular Sciences and Chemical Engineering* (Elsevier, 2019).

[5] D. V. Semenok, I. A. Kruglov, I. A. Savkin, A. G. Kvashnin, and A. R. Oganov, *On distribution of superconductivity in metal hydrides*, Current Opinion in Solid State and Materials Science **24**, 100808 (2020).

[6] D. Defang, L. Yunxian, T. Fubo, L. Da, H. Xiaoli, Z. Zhonglong, Y. Hongyu, L. Bingbing, T. Wenjing, and C. Tian, *Pressure-induced metallization of dense (h2s)2h2 with high-tc superconductivity*, Scientific Reports **4** (2014).

[7] H. Liu, I. I. Naumov, R. Hoffmann, N. W. Ashcroft,

and R. J. Hemley, *Potential high-tc superconducting lanthanum and yttrium hydrides at high pressure*, Proceedings of the National Academy of Sciences **114**, 6990–6995 (2017).

[8] H. Wang, J. S. Tse, K. Tanaka, T. Iitaka, and Y. Ma, *Superconductive sodalite-like clathrate calcium hydride at high pressures*, Proceedings of the National Academy of Sciences **109**, 6463–6466 (2012).

[9] A. P. Drozdov, M. I. Eremets, I. A. Troyan, V. Ksenofontov, and S. I. Shylin, *Conventional superconductivity at 203 kelvin at high pressures in the sulfur hydride system*, Nature, Letter **525**, 73–76 (2015).

[10] M. Einaga, M. Sakata, T. Ishikawa, K. Shimizu, M. I. Eremets, A. P. Drozdov, I. A. Troyan, N. Hirao, and Y. Ohishi, *Crystal structure of the superconducting phase of sulfur hydride*, Nature Physics **12** (2016).

[11] I. Osmond, O. Moulding, S. Cross, T. Muramatsu, A. Brooks, O. Lord, T. Fedotenko, J. Buhot, and S. Friedemann, *Clean-limit superconductivity in* $im\overline{3}mh_3S$ *synthesized from sulfur and hydrogen donor ammonia borane*, Phys. Rev. B **105**, L220502 (2022).

[12] A. P. Drozdov, P. P. Kong, V. S. Minkov, S. P. Besedin, M. A. Kuzovnikov, S. Mozaffari, L. Balicas, F. Balakirev, D. Graf, V. B. Prakapenka, E. Greenberg, D. A. Knyazev, M. Tkacz, and M. I. Eremets, *Superconductivity at 250 k in lanthanum hydride under high pressures*, Nature **569**, 528–531 (2019).

[13] M. Somayazulu, M. Ahart, A. K. Mishra, Z. M. Geballe, M. Baldini, Y. Meng, V. V. Struzhkin, and R. J. Hemley, *Evidence for superconductivity above 260 k in lanthanum superhydride at megabar pressures*, Phys. Rev. Lett. **122**, 027001 (2019).

[14] E. Snider, N. Dasenbrock-Gammon, R. McBride, X. Wang, N. Meyers, K. V. Lawler, E. Zurek, A. Salamat, and R. P. Dias, *Synthesis of yttrium superhydride superconductor with a transition temperature up to 262 k by catalytic hydrogenation at high pressures*, Phys. Rev. Lett. **126**, 117003 (2021).

[15] P. Kong, V. S. Minkov, M. A. Kuzovnikov, A. P. Drozdov, S. P. Besedin, S. Mozaffari, L. Balicas, F. F. Balakirev, V. B. Prakapenka, S. Chariton, D. A. Knyazev, E. Greenberg, and M. I. Eremets, *Superconductivity up to 243k in the yttrium-hydrogen system under high pressure*, Nature Communications **12** (2021).

[16] Y. Wang, K. Wang, Y. Sun, L. Ma, Y. Wang, B. Zou, G. Liu, M. Zhou, and H. Wang, *Synthesis and superconductivity in yttrium superhydrides under high pressure*, Chinese Physics B **31**, 106201 (2022).

[17] L. Ma, K. Wang, Y. Xie, X. Yang, Y. Wang, M. Zhou, H. Liu, X. Yu, Y. Zhao, H. Wang, G. Liu, and Y. Ma, *High-temperature superconducting phase in clathrate calcium hydride* cah_6 *up to 215 k at a pressure of 172 gpa*, Phys. Rev. Lett. **128**, 167001 (2022).

[18] E. Snider, N. Dasenbrock-Gammon, R. McBride, M. Debessai, H. Vindana, K. Vencatasamy, K. V. Lawler, A. Salamat, and R. P. Dias, *Room-temperature superconductivity in a carbonaceous sulfur hydride*, Nature **586**, 373–377 (2020).

[19] E. Snider, N. Dasenbrock-Gammon, R. McBride, M. Debessai, H. Vindana, K. Vencatasamy, K. V. Lawler, A. Salamat, and R. P. Dias, *Retraction note: Room-temperature superconductivity in a carbonaceous sulfur hydride*, Nature **610**, 804 (2022).

[20] E. J. Nicol and J. P. Carbotte, *Comparison of pressurized sulfur hydride with conventional superconductors*, Phys. Rev. B **91**, 220507 (2015).

[21] A. P. Durajski and R. Szczęśniak, *First-principles study of superconducting hydrogen sulfide at pressure up to 500 gpa*, Scientific Reports **7** (2017).

[22] D. A.P., S. R., and P. L., *High-temperature study of superconducting hydrogen and deuterium sulfide*, Annalen der Physik **528**, 358–364 (2015).

[23] I. Errea, M. Calandra, C. J. Pickard, J. Nelson, R. J. Needs, Y. Li, H. Liu, Y. Zhang, Y. Ma, and F. Mauri, *High-pressure hydrogen sulfide from first principles: A strongly anharmonic phonon-mediated superconductor*, Phys. Rev. Lett. **114**, 157004 (2015).

[24] R. Szczęśniak and A. P. Durajski, *Unusual sulfur isotope effect and extremely high critical temperature in h3s superconductor*, Scientific Reports **8** (2018).

[25] A. P. Durajski, *Quantitative analysis of nonadiabatic effects in dense h3s and ph3 superconductors*, Scientific Reports **6** (2016).

[26] H. Cui, M. Li, F. Zheng, and P. Zhang, *van hove singularities and tight-binding model in high-temperature superconductor h3se*, Physics Letters A **381**, 2526 – 2530 (2017).

[27] J. A. Flores-Livas, A. Sanna, and E. K. Gross, *High temperature superconductivity in sulfur and selenium hydrides at high pressure*, The European Physical Journal B **89**, 63 (2016).

[28] R. Szczesniak and A. Durajski, *The isotope effect in {H3S} superconductor*, Solid State Communications **249**, 30 – 33 (2017).

[29] W. Sano, T. Koretsune, T. Tadano, R. Akashi, and R. Arita, *Effect of van hove singularities on high-*T_c *superconductivity in* h_3S, Phys. Rev. B **93**, 094525 (2016).

[30] Y. Quan and W. E. Pickett, *Van hove singularities and spectral smearing in high-temperature superconducting* h_3S, Phys. Rev. B **93**, 104526 (2016).

[31] T. Skoskiewicz, A. W. Szafranski, W. Bujnowski, and B. Baranowski, *Isotope effect in the superconducting palladium-hydrogen-deuterium system*, Journal of Physics C: Solid State Physics **7**, 2670 (1974).

[32] C. Heil, S. di Cataldo, G. B. Bachelet, and L. Boeri, *Superconductivity in sodalite-like yttrium hydride clathrates*, Phys. Rev. B **99**, 220502 (2019).

[33] M. I. Eremets, V. S. Minkov, A. P. Drozdov, P. P. Kong, V. Ksenofontov, S. I. Shylin, S. L. Budko, R. Prozorov, F. F. Balakirev, D. Sun, S. Mozaffari, and L. Balicas, *High-temperature superconductivity in hydrides: Experimental evidence and details*, Journal of Superconductivity and Novel Magnetism **35** (2022).

[34] D. Sun, V. S. Minkov, S. Mozaffari, Y. Sun, Y. Ma, S. Chariton, V. B. Prakapenka, M. I. Eremets, L. Balicas, and F. F. Balakirev, *High-temperature superconductivity on the verge of a structural instability in lanthanum superhydride*, Nature Communications **12**, 6863 (2021).

[35] I. A. Troyan, D. V. Semenok, A. G. Kvashnin, A. V. Sadakov, O. A. Sobolevskiy, V. M. Pudalov, A. G. Ivanova, V. B. Prakapenka, E. Greenberg, A. G. Gavriliuk, I. S. Lyubutin, V. V. Struzhkin, A. Bergara, I. Errea, R. Bianco, M. Calandra, F. Mauri, L. Monacelli, R. Akashi, and A. R. Oganov, *Anomalous high-temperature superconductivity in yh6*, Advanced Materials **33**, 2006832 (2021).

[36] V. L. Ginzburg and L. D. Landau, *On the theory of superconductivity*, Zh. Eksp. Teor. Fiz. **20**, 1064–1082 (1950).

[37] N. R. Werthamer, E. Helfand, and P. C. Hohenberg, *Temperature and purity dependence of the superconducting critical field, H_{c2}. iii. electron spin and spin-orbit effects*, Phys. Rev. **147**, 295–302 (1966).

[38] J. Bardeen, L. N. Cooper, and J. R. Schrieffer, *Theory of superconductivity*, Phys. Rev. **108**, 1175–1204 (1957).

[39] J. E. Hirsch and F. Marsiglio, *Nonstandard superconductivity or no superconductivity in hydrides under high pressure*, Phys. Rev. B **103**, 134505 (2021).

[40] J. Hirsch and F. Marsiglio, *Meissner effect in nonstandard superconductors*, Physica C: Superconductivity and its Applications **587**, 1353896 (2021).

[41] J. E. Hirsch and F. Marsiglio, *Clear evidence against superconductivity in hydrides under high pressure*, Matter and Radiation at Extremes **7**, 058401 (2022), https://doi.org/10.1063/5.0091404.

[42] M. Dogan and M. L. Cohen, *Anomalous behavior in high-pressure carbonaceous sulfur hydride*, Physica C: Superconductivity and its Applications **583**, 1353851 (2021).

[43] G. M. Eliashberg, *Interaction between electrons and lattice vibrations in a superconductor*, J. Exptl. Theoret. Phys. **38**, 966–976 (1960).

[44] W. Kohn and L. J. Sham, *Self-consistent equations including exchange and correlation effects*, Phys. Rev. **140**, A1133–A1138 (1965).

[45] P. G. et al., *Quantum espresso: a modular and open-source software project for quantum simulations of materials*, Journal of Physics: Condensed Matter **21**, 395502 (2009).

[46] S. Baroni, S. de Gironcoli, A. Dal Corso, and P. Giannozzi, *Phonons and related crystal properties from density-functional perturbation theory*, Rev. Mod. Phys. **73**, 515–562 (2001).

[47] J. P. Perdew, K. Burke, and M. Ernzerhof, *Generalized gradient approximation made simple*, Phys. Rev. Lett. **77**, 3865–3868 (1996).

[48] D. R. Hamann, *Optimized norm-conserving vanderbilt pseudopotentials*, Phys. Rev. B **88**, 085117 (2013).

[49] M. van Setten, M. Giantomassi, E. Bousquet, M. Verstraete, D. Hamann, X. Gonze, and G.-M. Rignanese, *The pseudodojo: Training and grading a 85 element optimized norm-conserving pseudopotential table*, Computer Physics Communications **226**, 39–54 (2018).

[50] S. Baroni, P. Giannozzi, and E. Isaev, *Density-Functional Perturbation Theory for Quasi-Harmonic Calculations*, Reviews in Mineralogy and Geochemistry **71**, 39–57 (2010).

[51] M. A. Olea-Amezcua, O. De la Peña Seaman, and R. Heid, *Superconductivity by doping in alkali-metal hydrides without applied pressure: An ab initio study*, Phys. Rev. B **99**, 214504 (2019).

[52] P. B. Allen and R. C. Dynes, *Transition temperature of strong-coupled superconductors reanalyzed*, Phys. Rev. B **12**, 905–922 (1975).

[53] P. B. Allen, *Neutron spectroscopy of superconductors*, Phys. Rev. B **6**, 2577–2579 (1972).

[54] P. B. Allen and R. Silberglitt, *Some effects of phonon dynamics on electron lifetime, mass renormalization, and superconducting transition temperature*, Phys. Rev. B **9**, 4733–4741 (1974).

[55] J. M. Daams, J. P. Carbotte, and R. Baquero, *Critical field and specific heat of superconducting tl-pb-bi alloys*, Journal of Low Temperature Physics **35**, 547–559 (1979).

[56] S. Villa-Corts and O. De la Pea-Seaman, *Effect of van hove singularity on the isotope effect and critical temperature of h3s hydride superconductor as a function of pressure*, Journal of Physics and Chemistry of Solids **161**, 110451 (2022).

[57] S. Villa-Cortés and R. Baquero, *The thermodynamics and the inverse isotope effect of superconducting palladium hydride compounds under pressure*, Journal of Physics and Chemistry of Solids **123**, 371 – 377 (2018).

[58] S. Villa-Cortés and R. Baquero, *On the calculation of the inverse isotope effect in pdh(d): A migdal-eliashberg theory approach*, Journal of Physics and Chemistry of Solids **119**, 80 – 84 (2018).

[59] See Supplemental Material and references therein at [URL will be inserted by publisher] for technical details of the DFT and Density Functional Perturbation Theory, as well as the ME formalism used to get the superconducting properties.

[60] G. Bergmann and D. Rainer, *The sensitivity of the transition temperature to changes in $\alpha 2f(\omega)$*, Zeitschrift für Physik **263**, 59–68 (1973).

[61] S. Lie and J. Carbotte, *Dependence of tc on electronic density of states*, Solid State Communications **26**, 511 – 514 (1978).

[62] D. Rainer and F. J. Culetto, *Theory of the isotope effect in superconducting compounds: Pdd and* mo_6se_8, Phys. Rev. B **19**, 2540–2547 (1979).

[63] C. Leavens, *Calculations of the superconducting isotope effect*, Solid State Communications **15**, 1329 – 1332 (1974).

[64] G. Eilenberger and V. Ambegaokar, *Bulk (H_{c2}) and surface (H_{c3}) nucleation fields of strong-coupling superconducting alloys*, Phys. Rev. **158**, 332–339 (1967).

[65] K. D. Usadel, *Parameter $\kappa_2(t)$ for strong coupling superconducting alloys*, Phys. Rev. B **2**, 135–140 (1970).

[66] N. R. Werthamer and W. L. McMillan, *Temperature and purity dependence of the superconducting critical field H_{c2}. iv. strong-coupling effects*, Phys. Rev. **158**, 415–417 (1967).

[67] D. Rainer and G. Bergmann, *Temperature dependence of hc_2 and κ_1 in strong coupling superconductors*, Journal of Low Temperature Physics **14**, 501–519 (1974).

[68] K. Maki, *The magnetic properties of superconducting alloys i*, Physics Physique Fizika **1**, 21–30 (1964).

[69] S. B. Nam, *Theory of electromagnetic properties of superconducting and normal systems. i*, Phys. Rev. **156**, 470–486 (1967).

[70] S. B. Nam, *Theory of electromagnetic properties of strong-coupling and impure superconductors. ii*, Phys. Rev. **156**, 487–493 (1967).

[71] T. R. Lemberger, D. M. Ginsberg, and G. Rickayzen, *Calculation of the electromagnetic coherence length in superconductors with magnetic impurities*, Phys. Rev. B **18**, 6057–6065 (1978).

[72] J. P. Carbotte, *Properties of boson-exchange superconductors*, Rev. Mod. Phys. **62**, 1027–1157 (1990).

[73] V. H. J. and S. J. W., *Solving the eliashberg equations by means of n-point pade approximants*, Journal of Low Temperature Physics **29**, 179–192 (1977).